Effects of Surface Improvement Agent Composed of Lithium Silicate on Permeability and Durability of Hardened Concrete

T. Nawa[1], M. Suzuki[1], H. Naganuma[1], K. Kurumisawa[1]
[1]*Graduate school of engineering, Hokkaido University, Sapporo, Japan*

Abstract

Weakened surfaces of a concrete structure readily allow deteriorative substances into the concrete. Surface improvement agents have been developed for application to concrete surfaces to improve their surface properties, but most have reached few millimeters into concrete. In this study, we developed a new surface improvement agent primarily composed of lithium silicate. The experimental results indicated that this agent can penetrate into conventional concrete with W/C of 0.5 about 40mm in depth, and enhances the resistance to permeability as well as resistance of concrete to diffusion of chloride ion and freeze-thaw action.

1. Introduction

Improvement in the durability of concrete structures can lengthen the life of the structures. Hence, it has been of great significance from viewpoint of environmental protection and saving resources that are one of the most important issues.
Surface of reinforced concrete is a vital portion that can protect the structure from aggressive substances such as carbon dioxide and chloride ions, and from external impacts such as freezing and thawing action. The ingress of carbon dioxide and chloride accelerate the reinforcement corrosion, and freezing and thawing action cause the frost damage of concrete. Being exposed to the environment, however, surface of concrete is simultaneously deteriorated by cracking due to drying shrinkage and temperature changes, as well as by chemical erosion due to aggressive substances.

One of measures to strengthen and improve surface of concrete is applying surface improvement agent. This is intended to penetrate through concrete surfaces, generating gel material similar to cement hydrates, thereby densifying the subsurface microstructures [1]. However, there has been a problem of the depth of infiltration of such agents reaching only a few millimeters into the concrete. It is reported that such a thin layer of modification would scale off under freezing and thawing action, leaving a concrete surface more vulnerable to deterioration than untreated surfaces [2]. If the depth of infiltration is as large as 30 mm to 40mm, then it is considered that the concrete may possess

a excellent resistance to various deteriorative actions. In this study, the change in permeability with application of a new surface improvement agent primarily composed of lithium silicate was nvestigated, and the effect of its application on the durability of concrete was examined.

2. Properties and Application Method of Surface Improvement Agent

The newly developed surface improvement agent is primarily composed of lithium silicate combined with several alkaline compounds (hereafter referred to as LS). A conventional surface improvement agent that composes sodium/potassium silicate was also used for comparison (hereafter referred to as SC). Table 1 gives the physical and chemical properties of the surface improvement agents. The pH value of LS solution is lower than that of SC. However, it is possible that high pH of LS might promote alkali silica reaction. To confirm this, the potential alkali silica reaction of LS was examined by the mortar-bar method according to JIS A 1146. As a result, it was confirmed that the surface improvement agent did not promote the alkali silica reaction.

Table 1 Properties of surface improvement agents

Agent	Density /10^3 kg m^{-3}	pH
LS	1.10	11.7
SC	1.14	12.4

The surface improvement agent was applied to the moistened surfaces of specimens at 0.10 liter/m^2 (0.15 liter/m^2 for SC), and then was setting for 60 to 90 min. After that, a small amount of water was sprayed on the surface of specimens, and then another 0.1liter/m^2 of surface improvement agent was applied. The specimen was again setting more for 60 to 90 min.

3. Penetration of Surface Improvement Agent

3.1 Materials and Specimen Fabrication

In order to confirm the penetrability of LS, the inside of mortar specimen was observed using a scanning electron microscope (SEM). Normal cement mortar with water-cement ratio (W/C) of 0.6 and sand-cement ratio of 2.7 was fabricated. Mortar was poured into cylindrical specimens 50mm in diameter and 100 mm in length. At an age of 7 days, LS was applied only to the placing surfaces of the specimens. After moist curing, the specimens were axially cut at an age of 68 days.

3.2 Results and Discussion

Figure 1 shows a secondary electron image at 40mm depth from the surface. Figure 2 shows a secondary electron image of hydration products reacted with LS and saturated calcium hydroxide solution (hereafter referred to as LS gel). Similar needle-shaped products are observed in both images. Such products were not observed in untreated mortar, whereas they were marginally observed in mortar applied with SC at 0.5mm depth from the surface.

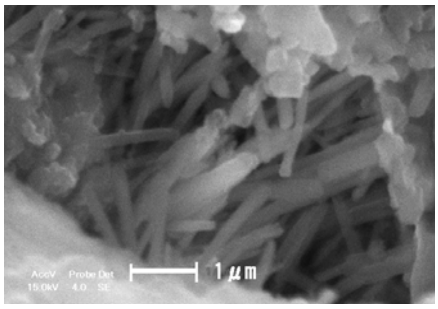

Fig.1 Secondary electron image of LS-treated mortar at 40mm depth

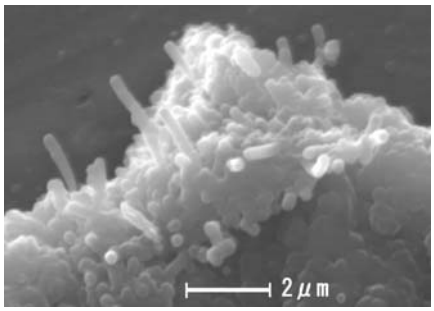

Fig.2 Secondary electron image of hydration products reacted with LS and saturated calcium hydroxide solution

The chemical composition of LS gel was examined by X-ray fluorescence analysis (XRF). Samples were prepared separating LS gel from the suspension centrifugally, washing the gel in ion exchanged water to remove unreacted Ca ions, and then drying. Tables 2 and 3 give the analysis results and the component ratios, respectively. As shown in Table 2, Li ions are not detected by XRF. Table 3 reveals that the Ca/Si ratio of LS gel is approximately half of that of C-S-H gel and that its Ca/Al ratio is 9 times as large as that of ettringite. It is therefore inferred that the LS gel shown in Fig. 2 differs from hydrates due to reaction between cement and water.

Table 2 Chemical composition of LS gel

Element	mass%	mol%
Al	0.64	0.79
Si	45.84	54.54
K	1.98	1.69
Ca	51.54	42.98

Table 3 Component of hydrates

Hydrates	Ca/Si	Ca/Al
C-S-H gel	1.5	N.A.
Ettringite	N.A.	6.0
LS gel	0.8	54.6

Accordingly, the needle-shaped products shown in Fig. 1 can be regarded as those formed by reaction between LS infiltrating into mortar and Ca ion in pore solution.

4. Effects of Surface Improvement Agent on Physical Properties and Durability of Mortar and Concrete

4.1 Materials and Sample Preparation

Ordinary Portland cement (OPC, density 3.16 gcm^{-3}, Blaine fineness 3320 cm^2g^{-1}) and Low-heat Portland cement (LH, density 3.22 gcm^{-3}, Blaine fineness 3500 cm^2g^{-1}) were used. Ground granulated blast furnace slag (GGBS, density 2.916 gcm^{-3}, surface area 6200 cm^2g^{-1}) was used as mineral admixture. Replacement of cement by GGBS was 50% by mass. Blended cement with OPC and GGBS is referred to as BB hereinafter. Crushed sandstone fine aggregate (Saturated-surface dry density 2.76 gcm^{-3}, water absorption 1.49%) and crushed sandstone coarse aggregate (Saturated-surface dry density 2.77 gcm^{-3}, water absorption 0.98%) were used. Lignosulfate based air entraining water-reducing admixture was employed as chemical admixture. The air-control agent was also used to control the air content.

Table 4 shows the mix proportions of concrete and mortar. Specimens were demoulded at age of 1 day and cured in water at 20°C until age of 14 days. After surface treatment, the specimens were cured at 20°C and 80% R.H. until the age of 28 days.

Table 4 Mix proportion of concrete and mortar

Symbol of specimen		Type of Cement	W/C	Air /%	s/a /%	Unit content/kg m^{-3} *			
						W	C	S	G
Concrete	OPC50	OPC	0.5	4.9	49	176	352	896	941
	BB50	BB	0.5	4.0	51	173	346	899	941
	LH30	LH	0.3	3.7	51	170	567	800	875
Mortar	OM50	OPC	0.5	6.0	-	275	550	1489	-
	OM60	OPC	0.6	2.5	-	295	491	1489	-

*W: Water, C: Cement, S: Fine aggregate , G: Coarse aggregate

4.2 Experimental Procedure

Permeability test by output method was carried out. OM60 mortar specimen 100mm in diameter and 200mm in length was used. After being sealed on the curved surface and treated only on the placing surface with the surface improvement agents, each specimen was moist-cured. The specimens were then transversely cut at 10mm intervals from the placing surfaces to measure the volume of water permeating under 0.1 MPa. The change in coefficient of permeability with depth was calculated by Eq. 1.

$$K_w = \frac{\omega h Q}{PA} \qquad (1)$$

where K_w permeability coefficient (m s^{-1})
P pressure (kgf m^{-2})
A cross-sectional area of specimen (m^2)
h thickness of specimen (m)
ω density of water (kg m^{-3})
Q volume of permeated water (m^3 s^{-1})

The effect of surface treatment on the ingress of chloride ion into concrete was investigated by chloride ion diffusion testing in accordance with JSCE-G571-2003. The effective diffusion coefficient of chloride ion was calculated from the flow velocity when the rate of increase in the chloride ion concentration on the anode side reached the steady state under applying a DC potential of 3 V across 10 mm thickness of specimen.
The deposition of LS gel within the pore in past forms the silica-rich layer on the pore wall, and gives a negative zeta potential. This effect was examined by a streaming potential measurement. Streaming potential measurement was carried out at a pressure step mode, that is , a certain pressure difference was applied to the system and allowed streaming potential to reach a constant value. Several pressure difference values were applied to determine the zeta potential. OPC and BB cement paste specimens, 100mm in diameter and 5mm in thickness, were used. The water-cement ratio was 0.5. Figure 3 shows the schematic of the test apparatus.

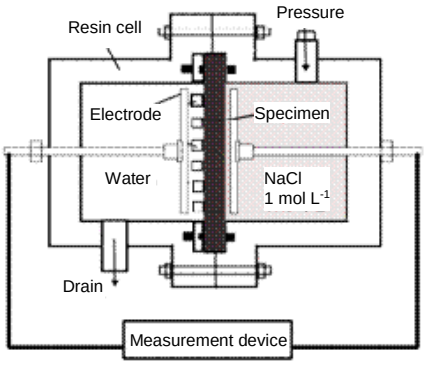

Fig. 3 Schematic of surface potential measurement test apparatus

Freezing and thawing test in water was conducted in accordance with procedure A of JIS A 1148 to examine the effect of the application of the agent on the frost resistance. OPC 50 and BB60 concretes were used for specimens. To investigate the effect of the agent on the frost resistance in a marine environment, tests were conducted in accordance with JIS A 1171 using OM50 mortar specimens immersed in seawater conforming to JIS A 6205.

4.3 Results and Discussion

4.3.1 Permeability

Figure 4 shows the permeability coefficient profiles along the depth from the surface. The coefficient of permeability of specimens with no surface modifier (described as “NO” in the figure) is the highest at 5mm from the surface, decreasing as the distance from the surface increases. This can be attributed to the fact that the water-cement ratio is the highest near the surfaces due to bleeding and settlement of cement particles and aggregate [3, 4].

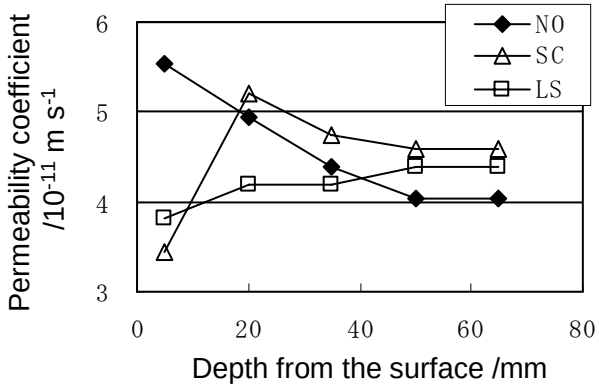

Fig. 4 Permeability coefficient profiles

In contrast, specimens with LS treatment showed slightly lower the permeability coefficient near the surface with no such significant changes over the depth as found in untreated specimens (NO). The permeability coefficient with LS is lower than that of NO specimens to a depth of around 40mm, coinciding with the depth to which the penetration of LS was confirmed in the previous section. Accordingly, the improvement effect of water-impermeability particularly near the surface is presumably brought about by the formation of hydrates within the mortar by the LS application.

In SC-treated specimens, the permeability coefficient is lower than in LS-treated specimens at 5mm from the surface, but being higher than untreated specimens at 20mm and deeper. This suggests that the range of densification by SC application is limited only to areas near the surface.

4.3.2 Chloride Shielding Property

Table 5 gives the effective diffusion coefficients of specimens with and without surface treatments. Figure 5 shows the ratios of effective diffusion coefficients of specimens with surface treatments to those of untreated specimens. It is evident that the effective diffusion coefficients of surface detective agent-treated specimens decrease in all mixture types, but the reductions vary depending on the agent type, W/C, and cement type.

Table 5 Effective diffusion coefficient /10^{-10} m^2 s^{-1}

Kind of mix proportion	Surface treatment		
	NO	SC	LS
OPC50	8.08	6.43	1.58
BB50	0.69	0.57	0.37
LH30	1.10	1.08	0.65

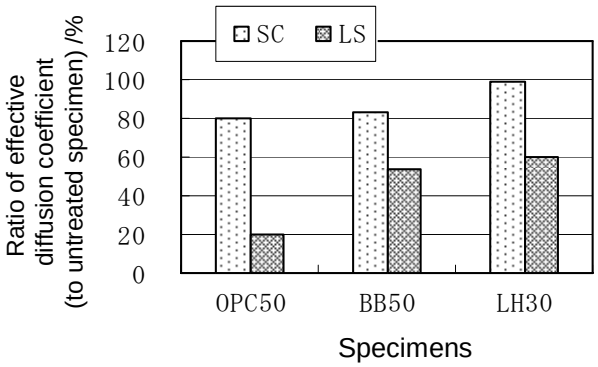

Fig. 5 Ratios of effective diffusion coefficients to those of untreated specimens

On the other hand, the effective diffusion coefficient of SC-treated specimens is 80 to 98% as low as that of untreated specimens. Further, LS-treated specimens shows 20 to 60% as low as that of untreated specimens, confirming the strong chloride shielding effect of LS. The diffusion coefficients of specimens made of BB50 and LH30 are substantially low due to the replacement by blast furnace slag and low water-cement ratio (0.3), respectively, even without treatment. However, the application of LS to these concrete reduced to even lower levels of 60% or less.

4.3.3 Zeta Potential

Figure 6 shows the changes in the zeta potential resulting from the surface treatments. The surface potential of OPC specimens without surface treatment is positive, but it turns significantly negative by the application of LS. BB specimens turns more negative by the LS application, though their zeta potentials are negative even without treatment.

The surface potential of cement paste is affected by the presence of Ca ions [5, 6]. The zeta potential of OPC specimens is positive due to the presence of Ca ion from $Ca(OH)_2$ generated by hydration, but that of BB specimens is more negative than that of OPC specimens because $Ca(OH)_2$ in BB specimens is consumed by hydration of blast furnace slag. The application of LS to these specimens enhances the formation of product hydrates, consuming Ca ions, thereby turning the potential much more negative.

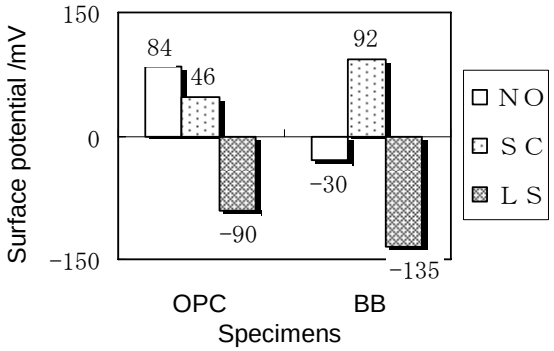

Fig. 6 Surface potential of cement pastes

The significantly negative potentials on hardened cement surfaces strongly inhibit the penetration of Cl ions by the electrostatic repulsion. This is presumably the reason for the strong chloride-shielding effect of LS application observed in the previous section.

On the other hand, the zeta potential of SC-treated BB specimens significantly turned positive, though that of SC-treated OPC specimens slightly turned negative. It is therefore difficult to relate

such potential changes to the effect of SC treatment on the chloride ion penetration. These results may reflect the sealing effect of SC by densification of only the surface areas.

4.3.4 Frost Resistance

Figure 7 (A) shows the durability factors of concrete specimens with or without the surface treatments. The durability factor of untreated OPC50 specimens is low at less than 60. This can be attributed to the small amount of available entrained air bubble. On the other hand, the durability factors of OPC50 and BB60 specimens treated with surface modifiers are significantly improved. The durability factors of LS-treated specimens particularly achieve nearly 100. This is confirmed the durability-improving effect of LS.

Figure 7 (B) shows the durability factors of mortar specimens with or without the surface modifiers in a marine environment. Untreated specimens rapidly deteriorated, resulting in a very low durability factor of 12. In contrast, the progress of deterioration was inhibited in treated specimens. The application of LS particularly improved the durability factor to as high as 69.

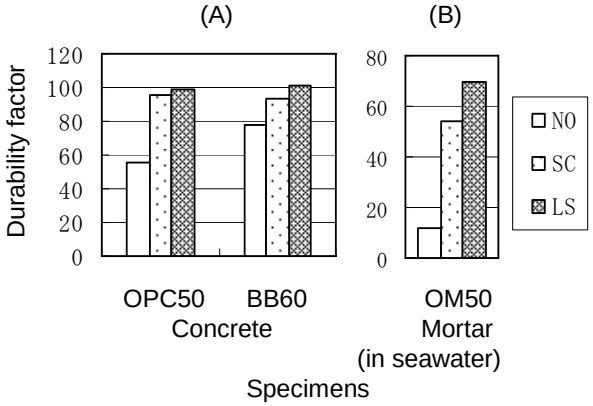

Fig. 7 Durability factors ; (A) concrete, (B) mortar specimens

Among the pictures of mortar placing surfaces at the end of 200-cycle testing shown in Fig. 8, the surface layer of the untreated specimen was completely peeled off by scaling. For SC-treated specimen, more than half the area of the surface layer was peeled off by scaling though its durability factor showed improvement. On the other hand, no marked scaling is observed on the LS-treated specimen, demonstrating an improvement in the scaling resistance.

Consequently, the application of LS is also found to have an effect of improving their resistance to freeze-thaw action.

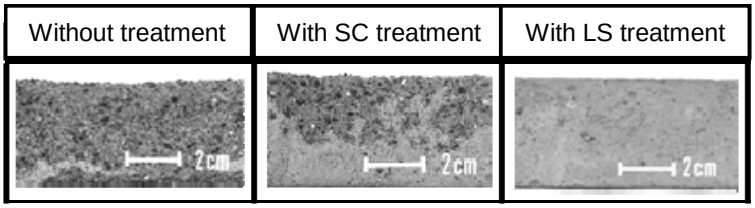

Fig. 8 Mortar placing surfaces at the end of 200-cycle

5. Conclusions

It was clarified that in mortar to which the new surface improvement agent was applied, needle-shaped products having forms similar to those reacted with this agent and $Ca(OH)_2$ were observed down to a depth of 40mm from the surface. The new surface improvement agent penetrates to a depth of nearly 40mm and generates hydrates presumably because the chemical compositions of the products formed by reaction with $Ca(OH)_2$ differ from those of normal cement hydrates.

The new surface improvement agent densified the microstructures by the products reacted with $Ca(OH)_2$, reducing the permeability coefficient in the range of 40mm from the surface. This effect was particularly significant near the surface.

The new surface modifier turned the potential negative on the surfaces of hardened cement by consuming $Ca(OH)_2$ for its reaction, thereby reducing the diffusion coefficient of Cl ions to 20 to 60%.

The durability factor of concrete to which the new surface improvement agent was treated was retained at 100, demonstrating a high resistance to frost damage. The scaling resistance of concrete was also improved by the new agent even in a marine environment.

References

[1] Present situation of techniques on surface coating and surface improvement of concretes: Japan Society of Civil Engineering, Japan, 2004, pp. 12-37
[2] H. Endoh, T. Taguchi, D. Hayashi, N. Sakata, Properties of scaling of concretes applied permeable antiabsorption agent (in Japanese) , Proceedings of the Japan Concrete Institute 26 (1) (2004) 987-992
[3] Kanda, M. and Yoshida, H., Distribution condition of water-cement ratio in the slab section after placing, Review of the 28th general meeting, The cement associate of Japan (1974)

104-106
[4] Kanda, M. and Yoshida, H., The distribution condition of water-cement ratio in the member section after concrete placing, Review of the 30th general meeting, The cement associate of Japan (1976) 168-170
[5] Skalny, J. and Young, J.F., Mechanisms of Portland cement hydration, Proc. 7th International Congress on the Chemistry of Cement, Paris, Vol.I (1984) II-1/3
[6] T. Nawa, H. Eguchi, M. Suzuki, Effect of pH on adsorption behavior of superplasticizer onto C_3A and C_4AF (in Japanese) , Cement Science and Concrete Technology 44 (1990) 80-85